Inorg. Chem. **2003**, *42*, 1140–1150

Tris(*tert*-butoxy)siloxy Derivatives of Boron, Including the Boronous Acid $HOB[OSi(O^tBu)_3]_2$ and the Metal (Siloxy)boryloxide Complex $Cp_2Zr(Me)OB[OSi(O^tBu)_3]_2$: A Remarkable Crystal Structure with 18 Independent Molecules in Its Asymmetric Unit

Kyle L. Fujdala,[†] Allen G. Oliver,*[,‡] Frederick J. Hollander,*[,‡] and T. Don Tilley*[,†]

Department of Chemistry, University of California, Berkeley, Berkeley, California 94720-1460, and Chemical Sciences Division, Lawrence Berkeley National Laboratory, 1 Cyclotron Road, Berkeley, California 94720-1460

Received September 10, 2002

Silanolysis of $B(O^tBu)_3$ with 2 and 3 equiv of $HOSi(O^tBu)_3$ led to the formation of $^tBuOB[OSi(O^tBu)_3]_2$ (**1**) and $B[OSi(O^tBu)_3]_3$ (**2**), respectively. Compounds **1** and **2** are efficient single-source molecular precursors to B/Si/O materials via thermolytic routes in nonpolar media, as demonstrated by the generation of $BO_{1.5}\cdot 2SiO_2$ (**BOSi2$_{xg}$**) and $BO_{1.5}\cdot 3SiO_2$ (**BOSi3$_{xg}$**) xerogels, respectively. Use of a block copolymer template provided B/Si/O materials (**BOSi2$_{epe}$** and **BOSi3$_{epe}$**) with a broad distribution of mesopores (by N_2 porosimetry) and smaller, more uniform particle sizes (by TEM) as compared to the nontemplated materials. Hydrolyses of **1** and **2** with excess H_2O resulted in formation of the expected amounts of ^tBuOH and $HOSi(O^tBu)_3$; however, reaction of **1** with 1 equiv of H_2O led to isolation of the new boronous acid $HOB[OSi(O^tBu)_3]_2$ (**3**). This ligand precursor is well suited for the synthesis of new metal (siloxy)boryloxide complexes via proton-transfer reactions involving the BOH group. The reaction of **3** with Cp_2ZrMe_2 resulted in formation of $Cp_2Zr(Me)OB[OSi(O^tBu)_3]_2$ (**4**) in high yield. This rare example of a transition metal boryloxide complex crystallizes in the triclinic space group $P\bar{1}$ and exhibits a crystal structure with an unprecedented number of independent molecules in its asymmetric unit (i.e., $Z' = 18$ and $Z = 36$). This unusual crystal structure presented an opportunity to perform statistical analyses of the metric parameters for the 18 crystallographically independent molecules. Complex **4** readily converts to $Cp_2Zr[OSi(O^tBu)_3]_2$ (**5**) upon thermolysis or upon dissolution in Et_2O at room temperature.

Introduction

The design and synthesis of advanced materials with tailored properties often requires low-temperature methods to permit the formation of metastable structures.[1] A widely used low-temperature approach for the synthesis of high surface area oxide materials is the sol−gel method.[2] This process involves the hydrolysis and condensation of one or more precursors, often alkoxides, in polar media (e.g., H_2O or ROH). Due to large differences in the hydrolysis rates of individual precursors, undesirable heterogeneous (poorly mixed) materials may form in sol−gel processes when multicomponent oxides are desired.[2] Although some degree of control is possible through the careful modification of each precursor, alternative methods that do not require added H_2O or polar media are useful for the preparation of highly homogeneous oxide materials.[3]

* To whom corrrespondence should be addressed. E-mail: tdtilley@socrates.berkeley.edu (T.D.T.).

[†] University of California and Lawrence Berkeley National Laboratory.

[‡] University of California College of Chemistry X-ray Crystallographic Facility (CHEXRAY).

(1) (a) *Ultrastructure Processing of Advanced Materials*; Uhlmann, D. R., Ulrich, D. R., Eds.; Wiley-Interscience: New York, 1992. (b) *Inorganic Materials*; Bruce, D. W., O'Hare, D., Eds.; Wiley: New York, 1992. (c) *Ceramic Precursor Technology and Its Applications*; Narula, C. K., Ed.; Marcel Dekker Inc.: New York, 1995. (d) Mehrotra, R. C. *J. Non-Cryst. Solids* **1988**, *100*, 1. (e) Stein, A.; Keller, S. W.; Mallouk, T. E. *Science* **1993**, *259*, 1558. (f) Amabilino, D. B.; Stoddart, J. F. *Chem. Rev.* **1995**, *95*, 2725. (g) Bowes, C. L.; Ozin, G. A. *Adv. Mater.* **1996**, *8*, 13.

(2) (a) Brinker, C. J.; Scherer, G. W. *Sol−Gel Science*; Academic Press: Boston, MA, 1990. (b) *Sol−Gel Technology for Thin Films, Fibers, Preforms, Electronics, and Specialty Shapes*; Klein, L. C., Ed.; Noyes: Park Ridge, NJ, 1988. (c) Brinker, C. J. *J. Non-Cryst. Solids* **1988**, *100*, 31. (d) Schmidt, H. *J. Non-Cryst. Solids* **1988**, *100*, 51. (d) Schubert, U.; Hüsing, N.; Lorenz, A. *Chem. Mater.* **1995**, *7*, 2010. (e) Corriu, R. J. P.; Leclercq, D. *Angew. Chem., Int. Ed. Engl.* **1996**, *35*, 1421. (f) Schubert, U. *J. Chem. Soc., Dalton Trans.* **1996**, 3343.

10.1021/ic0205482 CCC: $25.00
Published on Web 01/24/2003

In this context, we have been investigating the structure and reactivity of complexes containing $OSi(O^tBu)_3$ and $O_2P(O^tBu)_2$ ligands of the general formula $L_nM[OSi(O^tBu)_3]_m$[4] and $L_nM[O_2P(O^tBu)_2]_m$[5] (where L_n = alkoxide, amide, alkyl, etc.). These oxygen-rich molecules are excellent single-source precursors[6] to homogeneous mixed-element M/Si/O and M/P/O oxide materials due to their clean thermal decompositions (in organic solvent or in the solid state) at low temperatures (<200 °C) via the elimination of isobutene and H_2O. In addition, these complexes serve as soluble molecular models for heterogeneous catalysts based on oxide-supported metal species.[4m]

With the *thermolytic molecular precursor* route firmly established as an efficient method for the preparation of homogeneous, bicomponent oxide materials, we have sought to extend this approach to homogeneous tri- and tetra-component oxide materials. In this context, we recently reported the first complex containing both $-OSi(O^tBu)_3$ *and* $-O_2P(O^tBu)_2$ ligands, $[(^tBuO)_3SiO]_2Al[(\mu\text{-}O)_2P(O^tBu)_2]_2Al(Me)OSi(O^tBu)_3$, and demonstrated its use as an efficient single-source molecular precursor to high surface area silicoaluminophosphate materials.[7] The development of general routes to complexes with three or more heteroelements (e.g., Al, P, and Si) appropriate for use in the thermolytic molecular precursor method should lead to new homogeneous oxide materials with unique properties. One approach for the synthesis of such complexes would involve a single ligand precursor containing two or more heteroelements.

The aim of the current study was to synthesize new molecules containing boron and the $-OSi(O^tBu)_3$ ligand for use as single-source molecular precursors to borosilicate materials. In addition, the development of a general route for the formation of metal (siloxy)boryloxide species (with $M-O-B-OSi(O^tBu)_3$ linkages) was desired. In 1971 Abe et al. reported that silanolysis of $B(O^nBu)_3$ with $HOSi(O^tBu)_3$ produced $(^nBuO)_2BOSi(O^tBu)_3$ and $(^nBuO)B[OSi(O^tBu)_3]_2$ as viscous oils.[8] To provide clean conversions to materials at low temperatures (via CH_2CMe_2 elimination), we targeted species containing only ^{t}BuO groups. This work has provided two new crystalline compounds, ^{t}BuOB[OSi$(O^tBu)_3]_2$ (**1**) and $B[OSi(O^tBu)_3]_3$ (**2**), that are efficient single-source molecular precursors to borosilicate materials via solution thermolyses.

The Power,[9,10] Chisholm,[11] Gibson,[12] and Serwatowski[13] groups have synthesized metal diarylboryloxide complexes containing $[OBAr_2]^-$ ligands (where Ar = 2,4,6-$Me_3C_6H_3$,[9−13] 2,4,6-$^iPr_3C_6H_2$,[10] and 2,4,6-$(CF_3)_3C_6H_2$[11]) using $HOBAr_2$ or $LiOBAr_2$ reagents. Additionally, complexes of Zn and Cd are known for the 9-BBN-9-O ligand (BBN = borabicyclo-[3.3.1]nonane).[14] Thus far, these $OBAr_2$ and 9-BBN-9-O groups are the only boryloxide ligands that have been observed to support transition metal boryloxide complexes.[9−12,14] Simple $(RO)_2BOH$ compounds do not appear to be stable and have only been observed as components of product mixtures derived from hydrolysis of orthoborates $B(OR)_3$.[15] To obtain a (siloxy)boryloxide ligand precursor containing a BOH linkage, hydrolysis of **1** with 1 equiv of H_2O was investigated, and this led to isolation of $HOB[OSi(O^tBu)_3]_2$ (**3**). This boronous acid is, to our knowledge, the first isolable compound containing a $HOB(OSi)_2$ moiety. Its reaction with Cp_2ZrMe_2 demonstrates the use of this compound in the synthesis of the first boryloxide complex with a $MOB(OR)_2$ core, $Cp_2Zr(Me)OB[OSi(O^tBu)_3]_2$ (**4**).

Results and Discussion

Synthesis of Boron Tris(*tert*-butoxy)siloxide Derivatives. The reaction of 2 equiv of $HOSi(O^tBu)_3$ with $B(O^tBu)_3$ as a neat mixture at 80 °C led to the formation of ^{t}BuOB[OSi$(O^tBu)_3]_2$ (**1**) (eq 1). Analytically pure colorless crystals of

(3) (a) Jansen, M.; Guenther, E. *Chem. Mater.* **1995**, *7*, 2110. (b) Vioux, A. *Chem. Mater.* **1997**, *9*, 2292.

(4) (a) McMullen, A. K.; Tilley, T. D.; Rheingold, A. L.; Geib, S. J. *Inorg. Chem.* **1989**, *28*, 3772. (b) McMullen, A. K.; Tilley, T. D.; Rheingold, A. L.; Geib, S. J. *Inorg. Chem.* **1990**, *29*, 2228. (c) Terry, K. W.; Tilley, T. D. *Chem. Mater.* **1991**, *3*, 1001. (d) Terry, K. W.; Gantzel, P. K.; Tilley, T. D. *Chem. Mater.* **1992**, *4*, 1290. (e) Terry, K. W.; Gantzel, P. K.; Tilley, T. D. *Inorg. Chem.* **1993**, *32*, 5402. (f) Terry, K. W.; Lugmair, C. G.; Gantzel, P. K.; Tilley, T. D. *Chem. Mater.* **1996**, *8*, 274. (g) Su, K.; Tilley, T. D.; Sailor, M. J. *J. Am. Chem. Soc.* **1996**, *118*, 3459. (h) Su, K.; Tilley, T. D. *Chem. Mater.* **1997**, *9*, 588. (i) Terry, K. W.; Lugmair, C. G.; Tilley, T. D. *J. Am. Chem. Soc.* **1997**, *119*, 9745. (j) Rulkens, R.; Tilley, T. D. *J. Am. Chem. Soc.* **1998**, *120*, 9959. (k) Lugmair, C. G.; Tilley, T. D. *Inorg. Chem.* **1998**, *37*, 764. (l) Terry, K. W.; Su, K.; Tilley, T. D.; Rheingold, A. L. *Polyhedron* **1998**, *17*, 891. (m) Rulkens, R.; Male, J. L.; Terry, K. W.; Olthof, B.; Khodakov, A.; Bell, A. T.; Iglesia, E.; Tilley, T. D. *Chem. Mater.* **1999**, *11*, 2966. (n) Coles, M. P.; Lugmair, C. G.; Terry, K. W.; Tilley, T. D. *Chem. Mater.* **2000**, *12*, 122. (o) Kriesel, J. W.; Sander, M. S.; Tilley, T. D. *Mater. Chem.* **2001**, *13*, 3554. (p) Kriesel, J. W.; Sander, M. S.; Tilley, T. D. *Adv. Mater.* **2001**, *13*, 331. (q) Kriesel, J. W.; Tilley, T. D. *J. Mater. Chem.* **2001**, *11*, 1081. (r) Fujdala, K. L.; Tilley, T. D. *Chem. Mater.* **2001**, *13*, 1817. (s) Lugmair, C. G.; Fujdala, K. L.; Tilley, T. D. *Chem. Mater.* **2002**, *14*, 888. (t) Fujdala, K. L.; Tilley, T. D. *Chem. Mater.* **2002**, *14*, 1376.

(5) (a) Lugmair, C. G.; Tilley, T. D.; Rheingold, A. L. *Chem. Mater.* **1997**, *9*, 339. (b) Lugmair, C. G.; Tilley, T. D. *Inorg. Chem.* **1998**, *37*, 1821. (c) Lugmair, C. G.; Tilley, T. D. *Inorg. Chem.* **1998**, *37*, 6304. (d) Lugmair, C. G.; Tilley, T. D.; Rheingold, A. L. *Chem. Mater.* **1994**, *6*, 1615.

(6) Selected references on the single-source precursor approach: (a) Hubert-Pfalzgraf, L. G. *New J. Chem.* **1987**, *11*, 663. (b) Cowley, A. H.; Jones, R. A. *Angew. Chem., Int. Ed. Engl.* **1989**, *28*, 1208. (c) Chaput, F.; Lecomte, A.; Dauger, A.; Boilot, J. P. *Chem. Mater.* **1989**, *1*, 167, 199. (d) Mehrotra, R. C. *J. Non-Cryst. Solids* **1990**, *121*, 1. (e) Apblett, A. W.; Warren, A. C.; Barron, A. R. *Chem. Mater.* **1992**, *4*, 167. (f) Chandler, C. D.; Roger, C.; Hampden-Smith, M. J. *Chem. Rev.* **1993**, *93*, 1205. (g) Bradley, D. C. *Polyhedron* **1994**, *13*, 1111. (h) Narula, C. K.; Varshney, A.; Riaz, U. *Chem. Vap. Deposition* **1996**, *2*, 13. (i) Altherr, A.; Wolfganger, H.; Veith, M. *Chem. Vap. Deposition* **1999**, *5*, 87.

(7) Fujdala, K. L.; Tilley, T. D. *J. Am. Chem. Soc.* **2001**, *123*, 10133.

(8) Kijima, I.; Yamamoto, T.; Abe, Y. *Bull. Chem. Soc. Jpn.* **1971**, *44*, 3193.

(9) Weese, K. J.; Bartlett, R. A.; Murray, B. D.; Olmstead, M. M.; Power, P. P. *Inorg. Chem.* **1987**, *26*, 2409.

(10) Chen, H.; Power, P. P.; Shoner, S. C. *Inorg. Chem.* **1990**, *30*, 2884.

(11) Chisholm, M. H.; Folting, K.; Haubrich, S. T.; Martin, J. D. *Inorg. Chim. Acta* **1993**, *213*, 17.

(12) (a) Gibson, V. C.; Redshaw, C.; Clegg, W.; Elsegood, M. R. J. *Polyhedron* **1997**, *16*, 2637. (b) Gibson, V. C.; Mastroianni, S.; White, A. J. P.; Williams, D. J. *Inorg. Chem.* **2001**, *40*, 826.

(13) Anulewicz-Ostrowska, R.; Lulinski, S.; Serwatowski, J.; Suwinska, K. *Inorg. Chem.* **2000**, *39*, 5763.

(14) Lulinski, S.; Madura, I.; Serwatowski, J.; Zachara, J. *Inorg. Chem.* **1999**, *38*, 4937.

(15) Steinfeldt, K.-P.; Heller, G. *Z. Naturforsch., B: Chem. Sci.* **1981**, *36B*, 691.

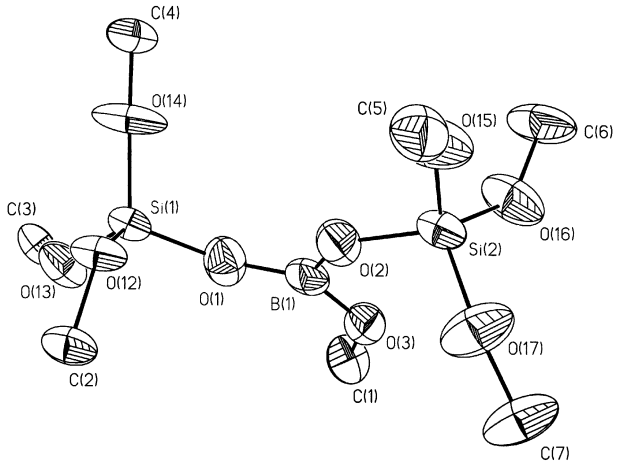

Figure 1. Thermal ellipsoid plot of **1** at the 50% probability level. The methyl groups have been omitted for clarity.

1 were isolated in 79% yield from a mixture of toluene and acetonitrile (4:1) at −30 °C.

$$B(O^tBu)_3 + 2HOSi(O^tBu)_3 \xrightarrow[-2^tBuOH]{80\ ^\circ C} (^tBuO)B[OSi(O^tBu)_3]_2 \quad \mathbf{1} \qquad (1)$$

A single-crystal X-ray crystallographic analysis revealed that molecules of **1** have a monomeric structure in the solid state (Figure 1). Compound **1** crystallizes in the triclinic space group $P\bar{1}$ with two molecules in the unit cell ($Z = 2$) and therefore one independent molecule in the asymmetric unit ($Z' = 1$). A summary of the crystallographic data is provided in Table 1, and selected bond distances and angles are listed in Table 2. Some of the methyl carbon atoms of the ^{t}Bu groups associated with the $OSi(O^tBu)_3$ ligands exhibited rotational disorder, and these were modeled over two positions with 50% occupancy and isotropic thermal parameters. All nondisordered C atoms and all O atoms were modeled using anisotropic thermal parameters. The boron atom is in a trigonal planar environment with the sum of the angles about the boron atom being 360.0(6)°. The B−O(C) (1.361(7) Å) and B−O(Si) (1.349(7) and 1.374(7) Å) bond distances are not significantly different from normal B−O distances (1.36 Å)[16] and are similar to the average B−O bond distances in $B(OSnPh_3)_3$ (1.368(6) Å),[17] $B(OSiPh_3)_3$ (1.357(4) Å),[18] $PhB(OGePh_3)_2$ (1.342(9) Å),[18] and $HOBMes_2$ (1.367(6) Å).[9] For further comparison, the structures of salen-supported borates containing phenylsiloxides have been recently reported by Atwood and coworkers.[19] These borates exhibit B−O(Si) distances (from 1.411(6) to 1.481(4) Å) that are significantly longer than those observed for the **1**. Presumably due to the steric strain induced by the bulky $OSi(O^tBu)_3$ ligands in compound **1**, the Si−O−B angles (141.8(4) and 136.7(4)°) are larger than the C−O−B angle (127.0(4)°). It is known that B−O−Si linkages are quite flexible and reported values for such angles range from ca. 129 to 161°.[18] The O−Si−O−B−O−Si−O linkage in **1** makes this compound an interesting molecular model for borosilicate materials, given that it is the first crystallographically characterized compound with such a linkage.

Table 1. Crystallographic Data for **1** and **4**

	^{t}BuOB[OSi(O^{t}Bu)$_3$]$_2$ (**1**)	Cp$_2$Zr(Me)OB[OSi(O^{t}Bu)$_3$]$_2$ (**4**)
formula	$C_{28}H_{63}BO_9Si_2$	$C_{35}H_{67}BO_9Si_2Zr$
cryst size (mm)	0.30 × 0.19 × 0.08	0.50 × 0.40 × 0.20
morphology	plate	tablet
cryst system	triclinic	triclinic
space group	$P\bar{1}$	$P\bar{1}$
Z, Z'	2, 1	36, 18
cell consts		
a (Å)	9.4639(3)	33.0365(5)
b (Å)	11.8965(2)	34.9417(6)
c (Å)	17.8225(7)	40.9629(6)
α (deg)	93.089(2)	103.134(1)
β (deg)	101.872(1)	92.809(1)
γ (deg)	101.340(2)	118.206(1)
V (Å^3)	1916.0(2)	39900(1)
D_{calc} (g cm^{-3})	1.059	1.184
F_{000}	672	15 192
μ(Mo Kα) (cm^{-1})	1.3	4.0
radiatn (λ, Å)	Mo Kα (0.710 69)	Mo Kα (0.710 69)
$2\theta_{max}$ (deg)	46.0	46.7
scan type	ω (0.3°/frame)	ω (0.3°/frame)
temp (°C)	−114	−118
exposure time	30 s/frame	40 s/frame
measd reflcns	8698	185 691
unique reflcns	5153	112 301
params/restr	351/0	7648/0
T_{max}/T_{min}	0.962/0.333	0.862/0.603
R_{int}	0.047	0.061
R_{obs}/R_{all}	0.083/0.136	0.067/0.163
$wR2_{obs}/wR2_{all}$	0.212/0.248	0.154/0.204
GOF_{obs}/GOF_{all}	1.127/0.983	0.943/0.943
max/min (e Å^{-3})	0.44/−0.37	1.13/−0.79

Attempts to prepare **1** in the presence of organic solvents (toluene, benzene, Et_2O) were met with reduced yields and the formation of significant amounts of a liquid product. Isolation of this new product in pure form was not achieved; however, ^{1}H NMR spectra of reaction mixtures suggested that it was $(^tBuO)_2BOSi(O^tBu)_3$. Reactions of 1 equiv of $HOSi(O^tBu)_3$ with $B(O^tBu)_3$ as a neat mixture or in solution also did not result in the clean isolation of this compound.

The reaction of 3 equiv of $HOSi(O^tBu)_3$with $B(O^tBu)_3$ in toluene at 80 °C resulted in the formation of $B[OSi(O^tBu)_3]_3$ (**2**) (eq 2). Analytically pure, colorless crystals were obtained in 61% overall yield by crystallization from a mixture of toluene and acetonitrile (4:1) at −30 °C. Despite many crystallization attempts, crystals of **2** were consistently of poor quality and not suitable for an X-ray crystallographic analysis. Given that **1** and the $B(OEPh_3)_3$ compounds[17,18] are monomeric in the solid state it is likely that **2** is also monomeric.

$$B(O^tBu)_3 + 3HOSi(O^tBu)_3 \xrightarrow[-3^tBuOH]{\text{toluene, } 80\ ^\circ C} B[OSi(O^tBu)_3]_3 \quad \mathbf{2} \qquad (2)$$

Hydrolyses of 1 and 2. The hydrolysis chemistry of **1** and **2** was investigated to characterize the utility of these

(16) Greenwood, N. N.; Earnshaw, A. *Chemistry of the Elements*; Pergamon: Oxford, England, 1984.
(17) Ferguson, G.; Spalding, T. R.; O′Dowd, A. T. *Acta Crystallogr., Sect. C* **1995**, *51*, 67.
(18) Murphy, D.; Sheehan, J. P.; Spalding, T. R.; Ferguson, G.; Lough, A. J.; Gallagher, J. F. *J. Mater. Chem.* **1993**, *3*, 1275.
(19) Wei, P.; Keizer, T.; Atwood, D. A. *Inorg. Chem.* **1999**, *38*, 3914.

Table 2. Selected Bond Distances (Å) and Angles (deg) for **1**

		Distances			
B(1)−O(1)	1.349(7)	Si(1)−O(14)	1.592(4)	O(12)−C(2)	1.457(6)
B(1)−O(2)	1.374(7)	Si(2)−O(2)	1.610(4)	O(13)−C(3)	1.436(6)
B(1)−O(3)	1.361(7)	Si(2)−O(15)	1.605(4)	O(14)−C(4)	1.413(6)
Si(1)−O(1)	1.610(4)	Si(2)−O(16)	1.601(4)	O(15)−C(5)	1.410(6)
Si(1)−O(12)	1.601(3)	Si(2)−O(17)	1.594(4)	O(16)−C(6)	1.383(6)
Si(1)−O(13)	1.590(4)	O(3)−C(1)	1.438(6)	O(17)−C(7)	1.407(6)
		Angles			
O(1)−B(1)−O(3)	123.4(6)	O(12)−Si(1)−O(1)	111.6(2)	B(1)−O(2)−Si(2)	136.7(4)
O(1)−B(1)−O(2)	120.0(5)	O(17)−Si(2)−O(16)	110.3(2)	B(1)−O(3)−C(1)	127.0(4)
O(3)−B(1)−O(2)	116.6(5)	O(17)−Si(2)−O(15)	108.9(2)	Si(1)−O(12)−C(2)	134.3(3)
O(13)−Si(1)−O(14)	109.3(2)	O(16)−Si(2)−O(15)	110.1(2)	Si(1)−O(13)−C(3)	136.3(3)
O(13)−Si(1)−O(12)	108.5(2)	O(17)−Si(2)−O(2)	110.4(2)	Si(1)−O(14)−C(4)	139.8(3)
O(14)−Si(1)−O(12)	110.4(2)	O(16)−Si(2)−O(2)	110.0(2)	Si(2)−O(15)−C(5)	136.3(4)
O(13)−Si(1)−O(1)	107.5(2)	O(15)−Si(2)−O(2)	107.1(2)	Si(2)−O(16)−C(6)	139.9(4)
O(14)−Si(1)−O(1)	109.5(2)	B(1)−O(1)−Si(1)	141.8(4)	Si(2)−O(17)−C(7)	140.4(4)

compounds as potential sol−gel precursors to borosilicate materials.[20] The reaction of 3 equiv of H_2O with **1** led to the rapid formation of ^{t}BuOH and $HOSi(O^tBu)_3$ (1 and 2 equiv, respectively), and the reaction of 3 equiv of H_2O with **2** led to the formation of 3 equiv of $HOSi(O^tBu)_3$. The formation of only $HOSi(O^tBu)_3$ (i.e., no ^{t}BuOH) from hydrolysis of **2** and the formation of only 1 equiv of ^{t}BuOH from hydrolysis of **1** (due to cleavage of the B−O^{t}Bu linkage) indicate that the B−O−Si linkages are much more susceptible to hydrolysis than are the Si−O^{t}Bu linkages. This indicates that the use of **1** or **2** in sol−gel procedures would lead to the preferential formation of B_2O_3 networks, with little initial incorporation of Si, thus leading to a heterogeneous material. This is not surprising given the well-known fact that B−O−Si linkages are unstable under typical sol−gel conditions, giving rise to heterogeneous B_2O_3/SiO_2 materials.[20]

Thermal Stability of 1 and 2. Thermogravimetric analysis (TGA) and differential scanning calorimetry (DSC) studies of **1** and **2** revealed that these species exhibit a melting transition (at ca. 70 and 160 °C for **1** and **2**, respectively) and subsequently boil (at ca. 170 and 255 °C for **1** and **2**, respectively) without thermal decomposition. Although boiling behavior has not been observed for metal complexes containing the $OSi(O^tBu)_3$ ligand,[4] $HOSi(O^tBu)_3$ displays similar melting and boiling behavior without thermal decomposition. The TGA and DSC results suggest that **1** and **2** will require a catalyst to facilitate their thermal conversions to borosilicate materials. For example, we have found that the thermal decomposition of $M[OSi(O^tBu)_3]_n$ complexes is acid catalyzed (e.g., HCl, $AlCl_3$)[4n,p] and that aluminosilicate materials catalyze the thermal decomposition of $HOSi(O^tBu)_3$.[4s]

Borosilicate Materials from 1 and 2. In light of the above observations, we elected to perform thermal decompositions of **1** and **2** in the presence of a small amount of $AlCl_3$ to determine the efficiency of these compounds as single-source molecular precursors to B/Si/O materials. Thermolyses of sealed tubes containing **1** or **2** dissolved in toluene at 180 °C in the presence of a catalytic amount of $AlCl_3$ (1 mol %) resulted in the formation of transparent monolithic gels that formed xerogels of composition $BO_{1.5}{\cdot}2SiO_2$ (**BOSi2$_{xg}$**) or $BO_{1.5}{\cdot}3SiO_2$ (**BOSi3$_{xg}$**) upon drying, respectively. The ceramic yields for **BOSi2$_{xg}$** (23.4%) and **BOSi3$_{xg}$** (25.8%) correspond closely to the expected yields (25.4% and 26.8%, respectively). Additional solution (toluene) thermolyses of **1** or **2** in the presence of the structure-directing block copolymer $EO_{20}PO_{70}EO_{20}$ (where EO = ethylene oxide and PO = propylene oxide) led to the mesoporous xerogels **BOSi2$_{epe}$** and **BOSi3$_{epe}$**, respectively, upon drying. It has previously been reported that use of this and related block copolymers have provided mesostructured oxide materials.[7,21] To our knowledge, these are the first examples of borosilicate materials obtained from single-source molecular precursors in nonpolar media.[20]

To characterize the chemistry involved in materials formation, the solution thermolyses of **1** and **2** were monitored using solution NMR spectroscopy by heating a toluene-d_8 solution of the precursor, $AlCl_3$ (∼1 mol %), and Cp_2Fe (as a standard) to 180 °C for 1 h in a sealed NMR tube. The major organic product detected in each case was CH_2CMe_2 with generation of only small amounts of ^{t}BuOH and trace amounts of $HOSi(O^tBu)_3$. This indicates that the thermolytic conversions of **1** and **2** proceed efficiently.[4,5,7]

Nitrogen porosimetry was used to characterize the surface areas and pore structures of the B/Si/O materials generated from **1** and **2** (Figure 2). The Brunnaur−Emmett−Teller (BET) method[22] was used to calculate the surface areas, and the Barrett−Joyner−Halenda (BJH) method[23] was used to obtain the pore size distributions. The surface area and pore

(20) (a) Irwin, A. D.; Holmgren, J. S.; Zerda, T. W.; Jonas, J. *J. Non-Cryst. Solids* **1987**, *89*, 191. (b) Irwin, A. D.; Holmgren, J. S.; Jonas, J. *J. Non-Cryst. Solids* **1988**, *101*, 249. (c) Zha, C.; Atkins, G. R.; Masters, A. F. *J. Non-Cryst. Solids* **1998**, *242*, 63. (d) Kasgöz, A.; Misono, T.; Abe, Y. *J. Non-Cryst. Solids* **1999**, *243*, 168. (d) Sorarù, G. D.; Babonneau, F.; Gervais, C.; Dallabona, N. *J. Sol-Gel Sci. Technol.* **2000**, *18*, 11. (e) Beckett, M. A.; Rugen-Hankey, M. P.; Varma, K. S. *Chem. Commun.* **2000**, 1499.

(21) For example: (a) Bagshaw, S. A.; Prouzet, E.; Pinnavaia, T. J. *Science* **1995**, *269*, 1242. (b) Attard, G. S.; Glyde, J. C.; Göltner, C. G. *Nature* **1995**, *378*, 366. (c) Göltner, C. G.; Antonietti, M. *Adv. Mater.* **1997**, *9*, 431. (d) Prouzet, E.; Pinnavaia, T. J. *Angew. Chem., Int. Ed. Engl.* **1997**, *36*, 516. (e) Zhao, D. Y.; Feng, J. L.; Huo, Q. S.; Melosh, N.; Fredrickson, G. H.; Chmelka, B. F.; Stucky, G. D. *Science* **1998**, *279*, 548. (f) Kriesel, J. W.; Sander, M. S.; Tilley, T. D. *Adv. Mater.* **2001**, *13*, 331.

(22) Brunauer, S.; Emmett, P. H.; Teller, E. *J. Am. Chem. Soc.* **1938**, *60*, 309.

(23) Barret, E. P.; Joyner, L. G.; Halenda, P. P. *J. Am. Chem. Soc.* **1951**, *73*, 373.

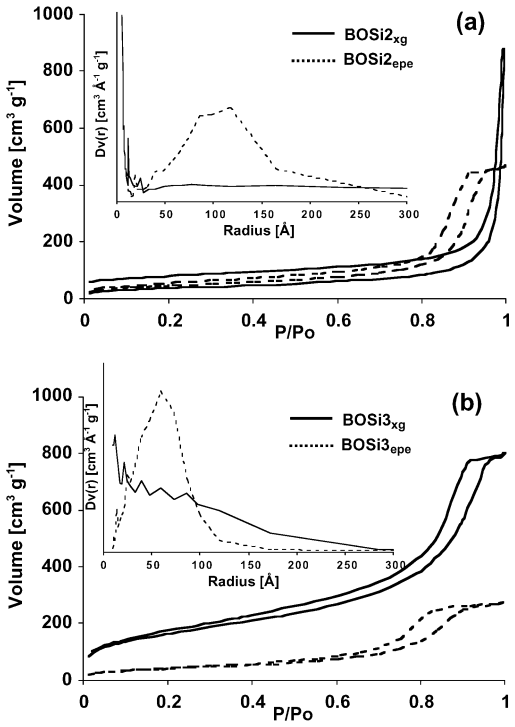

Figure 2. N_2 adsorption−desorption isotherms and pore size distributions (inset) after calcination at 500 °C for (a) **BOSi2$_{xg}$** and **BOSi2$_{epe}$** and (b) **BOSi3$_{xg}$** and **BOSi3$_{epe}$**.

volume data for **BOSi2$_{xg}$** (48 m^2 g^{-1} and 0.17 cm^3 g^{-1}) after calcination at 500 °C reveal a 1 order of magnitude (smaller) difference when compared to those of calcined **BOSi3$_{xg}$** (590 m^2 g^{-1} and 1.21 cm^3 g^{-1}). In contrast, the surface areas and pore volumes of **BOSi2$_{epe}$** (168 m^2 g^{-1} and 0.70 cm^3 g^{-1}) and **BOSi3$_{epe}$** (151 m^2 g^{-1} and 0.41 cm^3 g^{-1}) were quite similar. Thus, the presence of the copolymer appears to have a moderating effect on the pore structure and surface area. The pore size distributions as calculated from the adsorption branch of the adsorption−desorption isotherms revealed that **BOSi2$_{xg}$** and **BOSi3$_{xg}$** possess mostly pores with radii less than 10 Å, although larger pores were evident (Figure 2 insets). Analysis of the adsorption pore size distributions for **BOSi2$_{epe}$** and **BOSi3$_{epe}$** revealed a wide range of pore sizes in the mesoporous region (Figure 2 insets). The average pore radii as calculated using the BJH method and the adsorption (desorption) data for **BOSi2$_{epe}$** and **BOSi3$_{epe}$** were 118 Å (78 Å) and 59 Å (48 Å), respectively. Although the pore size distributions for **BOSi2$_{epe}$** and **BOSi3$_{epe}$** are not as narrow as those for other materials generated thermolytically in the presence of $EO_{20}PO_{70}EO_{20}$,[7,21f] their mesoporous nature is evident.

Transmission electron microscopy (TEM) studies revealed that the nontemplated xerogels (**BOSi2$_{xg}$** and **BOSi3$_{xg}$**) consisted of relatively large spherical particles of varying size (Figure 3). In contrast to this, the mesoporous borosilicates (**BOSi2$_{epe}$** and **BOSi3$_{epe}$**) exhibited significantly smaller particles with a more uniform size distribution (Figure 4). The presence of a wormhole-type motif is evident for both of these samples. Similar (although more ordered) wormhole structures have been previously observed by TEM for materials generated thermolytically from molecular

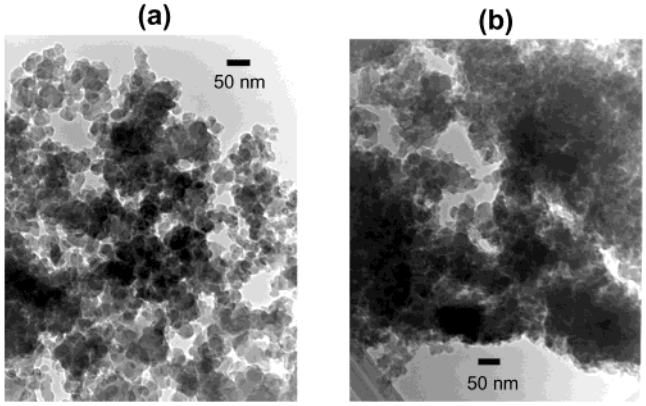

Figure 3. TEM micrographs of (a) **BOSi2$_{xg}$** and (b) **BOSi3$_{xg}$** after calcination at 500 °C.

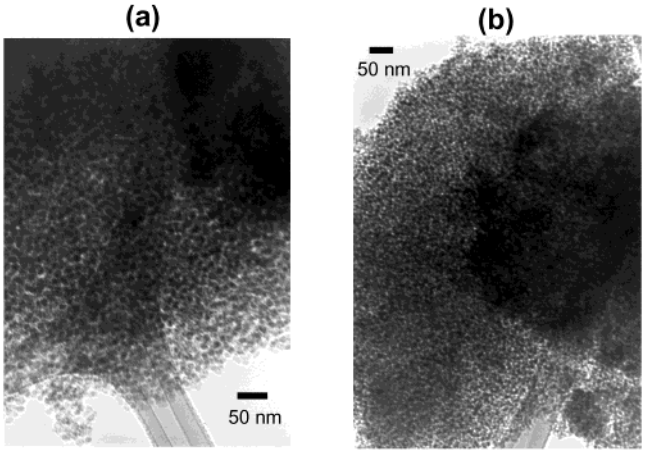

Figure 4. TEM micrographs of (a) **BOSi2$_{epe}$** and (b) **BOSi3$_{epe}$** after calcination at 550 °C.

precursors in the presence of block copolymers.[7,21f] The highly disordered nature of the pore structures for **BOSi2$_{epe}$** and **BOSi3$_{epe}$** likely arises from the structure-directing copolymer acting merely as an anisotropic space filler with little influence over the long-range ordering.[7,21]

Low-angle powder X-ray diffraction (PXRD) is often used to indicate the presence of mesostructural ordering with a single (well-defined) peak indicating a disordered structure with little long-range order and multiple peaks suggesting significant long-range order.[21] Such studies of the mesoporous B/Si/O materials (**BOSi2$_{epe}$** and **BOSi3$_{epe}$**) from $2\theta = 0.5$ to 3° revealed only a single broad feature originating at $2\theta = 0.9$ and 1.1° for **BOSi2$_{epe}$** and **BOSi3$_{epe}$**, respectively, and increasing in intensity to $2\theta = 0.5°$ (the start of the measurement). The ill-defined nature and broadness of these peaks suggest that there is no long-range mesostructural order and that the mesopores cover a wide size distribution.

Synthesis of the New Boronous Acid HOB[OSi(O^{t}Bu)$_3$]$_2$. Hydrolysis of **1** with only 1 equiv of H_2O in benzene-d_6 led to the appearance of two new resonances at 5.71 and 1.41 ppm in the ^{1}H NMR spectrum. Integration of these resonances suggested that this new species could be HOB[OSi(O^{t}Bu)$_3$]$_2$ (**3**, eq 3). Nearly quantitative amounts of **3** (by ^{1}H NMR spectroscopy and integration against a Cp_2Fe standard) were observed initially; however, slow

decomposition to insoluble material occurred over the course of a few hours.

$$(^t\mathrm{BuO})\mathrm{B}[\mathrm{OSi}(\mathrm{O}^t\mathrm{Bu})_3]_2 + \mathrm{H_2O} \xrightarrow[-{}^t\mathrm{BuOH}]{\text{benzene, 25 °C}} \underset{\mathbf{1}}{\mathrm{HOB}[\mathrm{OSi}(\mathrm{O}^t\mathrm{Bu})_3]_2} \quad (3)$$

3

Isolation of **3** was ultimately achieved by performing the reaction of **1** with 1 equiv of H_2O in benzene at 25 °C for 1 h. Subsequent freezing of the reaction mixture (at 0 °C) and removal of the solvent in vacuo (via lyophilization) allowed the isolation of a mixture of **3** and small amounts of **2** (ca. 5%) as a colorless powder. Sublimation of the powder at 50 °C in vacuo resulted in the isolation of analytically pure **3** in 86% yield. Attempts to isolate **3** from other solvents (toluene, Et_2O, THF, and pentane), either upon cooling (for crystallization) or upon concentration in vacuo, resulted in the decomposition of **3**. However, **3** is stable for several months in the solid state at room temperature. Although we were unable to crystallographically characterize **3**, its identity was confirmed by NMR (^{1}H, ^{13}C, and ^{11}B) and IR spectroscopies and combustion analysis (C and H). Attempts to prepare $HOB(O^tBu)_2$ via hydrolysis of $B(O^tBu)_3$ were hindered by rapid hydrolysis and condensation processes to form B_2O_3. The exclusive formation of **3** during the initial stages of the hydrolysis of **1** indicates that the B−O^{t}Bu linkages are significantly more susceptible to hydrolytic cleavage than are the B−OSi(O^{t}Bu)$_3$ fragments. Hence, it follows that the order of hydrolytic stability is B−O^{t}Bu < B−OSi ≪ Si−O^{t}Bu.

Synthesis of $Cp_2Zr(Me)OB[OSi(O^tBu)_3]_2$ (4). With the potential ligand precursor **3** in hand, we sought to explore its use as a reagent for synthesis of new boryloxide complexes of the type $L_xM\{OB[OSi(O^tBu)_3]_2\}_y$. The reaction of **3** with Cp_2ZrMe_2 in pentane at 25 °C resulted in the formation of $Cp_2Zr(Me)OB[OSi(O^tBu)_3]_2$ (**4**) (quantitative by ^{1}H NMR spectroscopy, eq 4). Colorless crystals of analytically pure **4** were isolated in 90% yield from a concentrated pentane solution at −78 °C. The crystals of **4** proved to be extremely moisture sensitive and exhibited a melting/decomposition transition at just above room temperature (ca. 30 °C). Complex **4** is stable in the presence of 1 equiv of **3** in benzene-d_6 solution for 2 h at 25 °C, after which time decomposition was evident.

$$\underset{\mathbf{3}}{\mathrm{HOB}[\mathrm{OSi}(\mathrm{O}^t\mathrm{Bu})_3]_2} + \mathrm{Cp_2ZrMe_2} \xrightarrow[-\mathrm{CH_4}]{\text{pentane, 25 °C}} \underset{\mathbf{4}}{\mathrm{Cp_2Zr}(\mathrm{Me})\mathrm{O{-}B}(\mathrm{OSi}(\mathrm{O}^t\mathrm{Bu})_3)_2} \quad (4)$$

This new boryloxide complex, containing both Zr−O−B and Zr-Me linkages, could serve as a molecular model for oxide-supported metallocene complexes.[24−26] The difficulties involved in identifying the structures of solid-supported organometallic fragments make the synthesis of well-defined molecular model complexes that mimic potential structures of grafted fragments (containing E−O−M linkages) highly desirable. In a recent investigation by Basset and co-workers on the nature of surface-bound species resulting from the grafting of $CpZrMe_3$ and Cp_2ZrMe_2 onto various Lewis acidic oxide materials (e.g., Al_2O_3 and Al_2O_3/SiO_2), structures with Zr−O surface linkages that closely resemble that of **4** were proposed.[25]

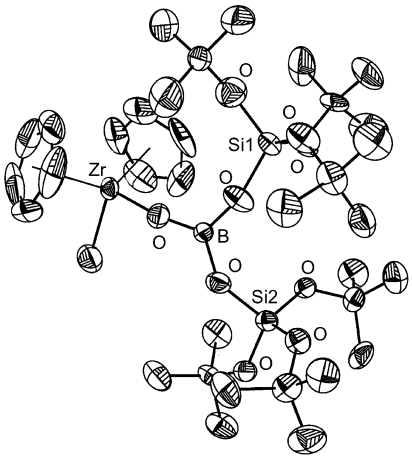

Figure 5. Thermal ellipsoid plot showing one unique molecule of **4** from the asymmetric unit at the 50% probability level. Si1 represents the Si atom farthest from the Zr−Me group. Hydrogen atoms have been omitted for clarity.

Structural Characterization of 4. Colorless crystals (tablets) of **4** that were of sufficient quality for an X-ray crystallographic analysis were grown from a concentrated pentane solution after storage at −30 °C for several weeks. Complex **4** crystallized in the triclinic space group $P\bar{1}$ with 36 molecules in the unit cell ($Z = 36$). This corresponds to 18 unique molecules in the asymmetric unit ($Z' = 18$), which we believe is the largest number of molecules ever observed in the asymmetric unit of a fully documented crystal structure. A thermal ellipsoid plot of one of the molecules from the asymmetric unit of **4** is shown in Figure 5, and a space-filling diagram of the entire asymmetric unit is shown in Figure 6.

A search of the Cambridge Structural Database (CSD, version 5.22, October 2001) for structures with $Z' \geq 16$ revealed only 6 compounds.[27] Of these, two structures (a diterpenoid[27d] and $HOSnMe_3$[27a]) had $Z' \geq 18$; however, no 3D coordinates were listed in the CSD so it was not possible to analyze the data independently. The information given in the original paper for the diterpenoid structure ($Z' = 20.5$)

(24) (a) Hlatky, G. G. *Coord. Chem. Rev.* **1999**, *181*, 243. (b) Hlatky, G. G. *Chem. Rev.* **2000**, *100*, 1347.

(25) Jezequel, M.; Dufaud, V.; Ruiz-Garcia, M. J.; Carrillo-Hermosilla, F.; Neugebauer, U.; Niccolai, G. P.; Lefebvre, F.; Bayard, F.; Corker, J.; Fiddy, S.; Evans, J.; Broyer, J.-P.; Malinge, J.; Basset, J.-M. *J. Am. Chem. Soc.* **2001**, *123*, 3520.

(26) Duchateau, R.; Cremer, U.; Harmsen, R. J.; Mohamud, S. I.; Abbenhuis, H. C. L.; van Santen, R. A.; Meetsma, A.; Thiele, S. K.-H.; van Tol, M. F. H.; Kranenburg, M. *Organometallics* **1999**, *18*, 5447.

(27) (a) Kasai, N.; Yasuda, K.; Okawara, R. *J. Organomet. Chem.* **1965**, *3*, 172. (b) Bruckner, S. *Acta Crystallogr., Sect. B* **1982**, *38*, 2405. (c) Hsu, L.-Y.; Nordman, C. E. *Science* **1983**, *220*, 604. (d) Hashimoto, T.; Toyota, M.; Koyama, H.; Kikkawa, A.; Yoshida, M.; Tanaka, M.; Takaoka, S.; Asakawa, Y. *Tetrahedron Lett.* **1998**, *39*, 579. (e) Hassaballa, H.; Steed, J. W.; Junk, P. C.; Elsegood, M. R. J. *Inorg. Chem.* **1998**, *37*, 4666. (f) Chou, S.-S. P.; Liu, S.-H. *J. Organomet. Chem.* **1998**, *555*, 227.

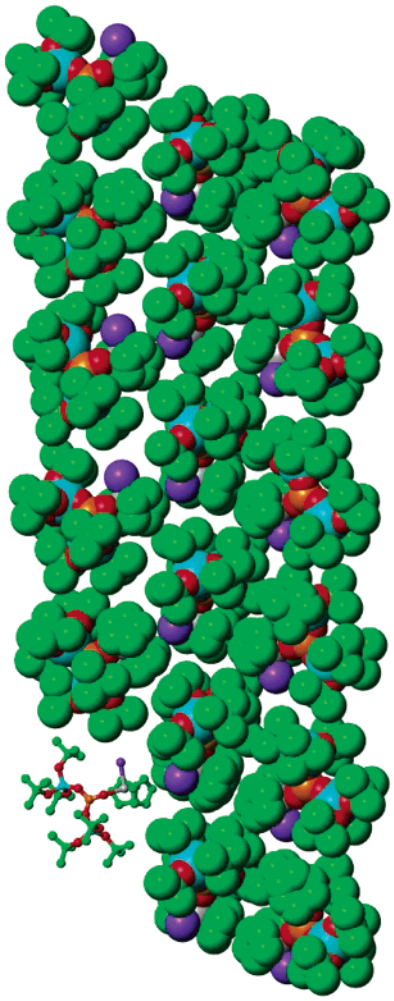

Figure 6. Space-filling diagram of the asymmetric unit for the crystal structure of **4** as generated from the crystallographic data.

is inconsistent and strongly suggests a typographical error in the cell parameter a ($a = 14.82$ Å rather than $a = 114.82$ Å as reported) and in the Z value ($Z = 8$ rather than $Z = 82$ reported).[27d] If these changes are made, the cell volume agrees with the reported volume (4357(1) Å^3) and a more reasonable Z' value of 2 is obtained. The structure of $HOSnMe_3$ ($Z' = 32$) was determined from a poor quality data set (232 observations), and the reported unit cell was an extension of a smaller subcell ($a = 2a'$ and $c = 2c'$).[27a] The extension to the larger unit cell was based upon 10 "very weak" reflections. The actual unit cell is likely one of the two given subcells (Pn, $Z = 16$, or $P2_1nm$, $Z = 2$).[27a] The only other metal-containing structures in the search results, $[UO_2(H_2O)_3Cl_2]\cdot$15-crown-5[27e] and tricarbonyl[(1−4-η^4)-6-exo-cyano-2-(phenylsulfonyl)-1,3-cyclohexadiene]iron,[27f] have $Z' = 16$.

Whenever an "unusual" or "unique" structure is determined, it is proper to consider whether the "uniqueness" is due to nature or is due to the failure of the experimenters to recognize other explanations for the results. While no such examination is foolproof, we did apply stringent tests to the crystallographic data obtained for **4**. The raw data (both CCD frames and derived structure factors) were repeatedly examined for unusual systematic absences, which might indicate a twinned crystal or a falsely determined cell. The data were also analyzed for twinning using the program "Gemini"[28] which again indicated no sign of twinning. Further, the cell determined in this analysis was the same as that found originally without the original being provided at the outset of the analysis.[29]

That this was not a unique crystal sample (an artifact of the "selection effect") is demonstrated by our observation of the same unit cell determined from four different crystals of varying quality selected from two different recrystallizations of complex **4** over the period of 1 month. The observation of the same unit cell for multiple crystals also suggests that crystal cracking is not responsible for the unusual nature of the structure. The cell and the structure were additionally subjected to the routines of MISSYM and ADDSYM in the PLATON suite of programs.[30] No additional symmetry or higher symmetry space group was found. Careful examination of each molecule in the asymmetric unit shows that each is in some way unique either in conformation or (equally important in a crystal structure) orientation.

Details of the data collection, structure solution, and refinement are provided in the Experimental Section and in Table 1. Seven of the molecules in the asymmetric unit exhibited rotational disorder in a single ^{t}Bu group, and this commonly observed ^{t}Bu disorder was modeled using two carbon atoms at 50% occupancy for each disordered Me group. Some of the O^{t}Bu oxygen atoms (18 out of 108) exhibited disorder, and this was modeled over two positions at 50% occupancy. The Cp rings of one of the molecules had positional disorder that was easily modeled over two sites with appropriate atoms at 50% occupancy. All other Cp ligands were normal. Remarkably, all 18 $MeZrOB(OSi)_2$ moieties were well behaved and contained no disordered atoms. The Zr, Si, and nondisordered C and O atoms were modeled with anisotropic thermal parameters. There are no significantly close intermolecular contacts (i.e., no "hydrogen bumping").

The nature of the crystal structure afforded a rare opportunity to perform detailed statistical analyses of the metric parameters with a large pool of independent molecules to analyze. The usual metric parameters (bond lengths and angles) show regular, normal distributions as would be expected if the data were correct and accurate. The disorder discussed above gives rise to a few outliers, which can be ignored for statistical purposes. Figure 7 presents the distribution of C−C bond distances and clearly shows a normal distribution for both the Cp and ^{t}Bu C−C bond lengths. The observed mean C−C bond distances are

(28) Sparks, R. A. *GEMINI*; Bruker-AXS, Inc.: Madison WI, 1999 (part of the SMART software suite).
(29) We thank Dr. Victor G. Young, Jr., Director, X-ray Crystallographic Facility, Department of Chemistry, University of Minnesota, for these analyses.
(30) Spek, A. L. *PLATON, a multipurpose crystallographic tool*; Utrecht University: Utrecht, The Netherlands, 2001. We thank Prof. Anthony L. Spek, Utrecht University, Utrecht, The Netherlands, for these analyses.

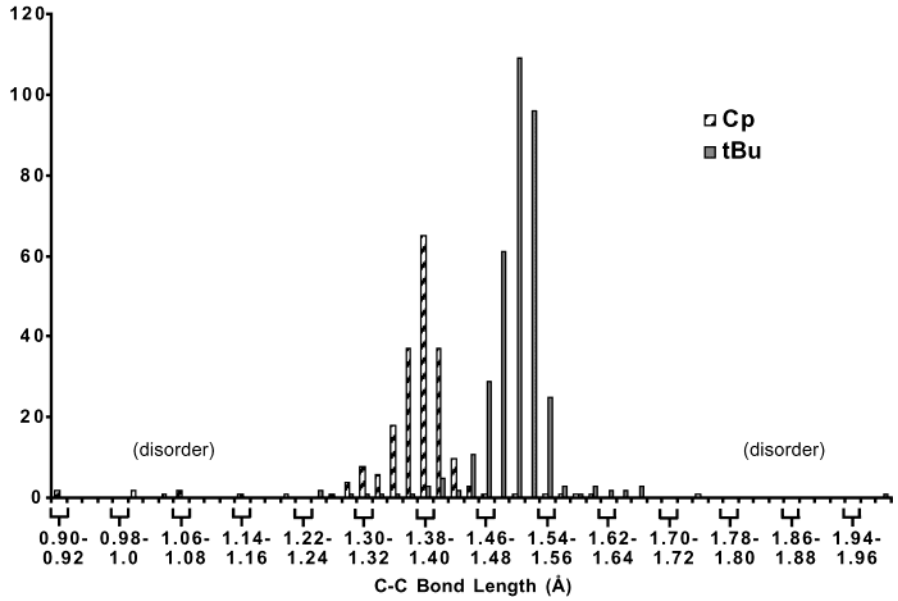

Figure 7. Plot of the distribution of C−C bond lengths for **4**. The space between *x*-axis tick marks corresponds to 0.02 Å. The outliers are due to disorder in the crystal structure.

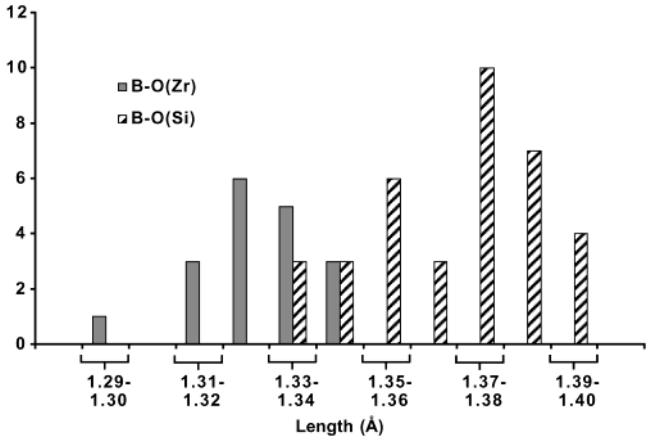

Figure 8. Plot of the distribution of B−O(Zr) and B−O(Si) bond lengths for **4**. The space between *x*-axis tick marks corresponds to 0.01 Å.

1.375(6) and 1.509(3) Å for the Cp and ^{t}Bu groups, respectively. Figure 8 shows the distribution of B−O bond distances and illustrates that the B−O(Zr) distances are generally shorter than the B−O(Si) distances. The mean B−O(Zr) distance is 1.329(3) Å, and the mean B−O(Si) distance is 1.370(3) Å with no significant difference between the B−O(Si1) and B−O(Si2) mean distances (1.364(3) and 1.377(3) Å), where Si1 corresponds to the siloxide group farthest from the Zr−CH_3 linkage in each molecule. The mean Si−O distance in **4** is 1.609(4) Å with no significant difference between Si(1)−O and Si(2)−O distances or between Si−O(C) and Si−O(B) distances. Table 3 provides a summary of the statistical analyses for selected bond distances and angles.

The mean O−B−O angle is 120.0(4)°, as would be expected for a trigonal planar boron center. The B−O−Si angles exhibit a wide range of values (from 133.2 to 164.0°); however, these approximate a (wide, tailed) normal distribution as shown in Figure 9. Interestingly, the Zr−O−B angles show an apparent trimodal distribution over a wide range of

Table 3. Bond Distance (Å) and Angle (deg) Statistics for **4**

	N	min value[a]	max. value[a]	mean value[b]
		Distances		
Zr−O	18	1.921	1.999	1.974(4)
Zr−C(CH_3)	18	2.250	2.297	2.281(3)
Zr−C(Cp)	180	2.474 (2.455)	2.566	2.520(2)
B−O(Zr)	18	1.296	1.345	1.329(3)
B−O(Si)	36	1.338	1.394	1.370(3)
Si−O(B)	36	1.534	1.637	1.604(3)
Si−O(C)	126	1.492 (1.398)	1.629 (1.813)	1.610(4)
C−O	126	1.398 (1.269)	1.490 (1.716)	1.460(5)
C−C(^{t}Bu)	362	1.402 (1.250)	1.586 (1.990)	1.509(3)
C−C(Cp)	203	1.292 (0.910)	1.450 (1.760)	1.375(6)
		Angles		
C(CH_3)−Zr−O	18	96.9	100.3	98.4(2)
Zr−O−B	18	146.5	177.5	160(2)
O−B−O	54	111.3	124.7	120.0(4)
B−O−Si	36	133.2	164.0	144(1)
O−Si−O	251	102.7 (84.6)	116.2 (138.8)	109.3(4)
Si−O−C	126	129.6 (118.7)	141.0 (151.7)	132.0(4)
C−C−C	549	104.2 (78.5)	113.2 (148.5)	109.9(2)

[a] The value in parentheses indicates a distance or angle involving a disordered atom. [b] Calculated using "*N*" parameters, including disorder where appropriate. Esd in parentheses.

values from 146.5 to 177.5° with a mean value of 160(2)° (Figure 9). Of the 36 Zr−O−B−O torsion angles that ranged from −180 to 180°, 9 were between −90 and −60°, another 9 were between 90 and 120°, and the rest were spread evenly within given 30° intervals. The net effect of the OB[OSi-(O^tBu)$_3$]$_2$ ligand appears to be a steric shrouding of the metal center in an umbrella-like fashion with the rather long Zr−O−B−O linkage as the handle. The Zr−Me group, however, is relatively unprotected in all observed conformations. The oxygen atom of the Zr−O−B linkage behaves as if it were a universal joint with a soft bending potential, allowing the tris(*tert*-butoxy)siloxide groups to assume many not-so-subtly different orientations relative to the Zr atom and the Cp groups. This appears to be a major factor in the crystallization of 18 independent molecules in the asymmetric unit (but does

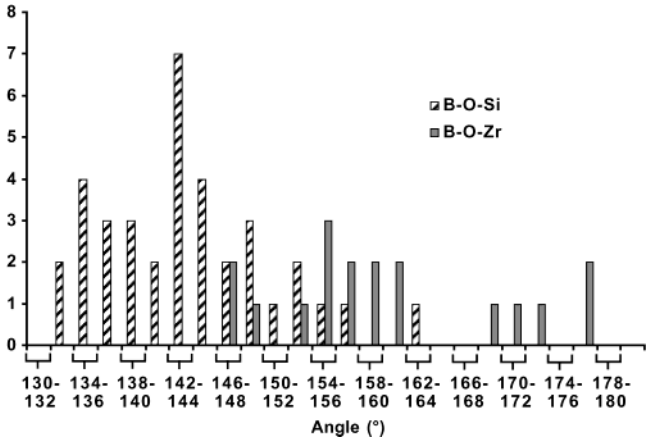

Figure 9. Plot of the distribution of Zr−O−B and Si−O−B angles for **4**. The space between *x*-axis tick marks corresponds to 2°.

Scheme 1

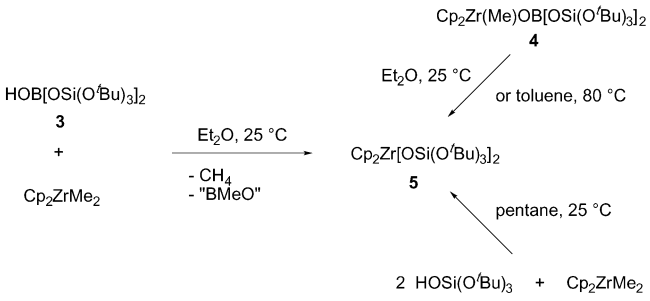

not explain *why* there are *18* molecules, nor does it describe the nature of the long-range ordering forces).

Complex **4** is a rare example of a crystallographically characterized transition metal boryloxide and is, to our knowledge, the first transition metal boryloxide with a $M-OB(OR)_2$ moiety. The other structurally characterized transition metal boryloxides are $[Co(\mu\text{-}OBMes_2)_2Li(THF)_2Cl_2$-$Li(THF)_2$,[9] $[Mn(OBTrip_2)(\mu\text{-}OBTrip_2)]_2$,[10] $[Fe(OBMes_2)(\mu$-$OBMes_2)]_2$,[10] $[(NMe_2)_2WOBMes_2]_2$,[11] $[(^tBuO)_2WOBMes_2]_2$,[11] $[(\mu^3\text{-}9\text{-}BBN\text{-}9\text{-}O)ZnEt]_4$,[14] and $[(\mu^3\text{-}9\text{-}BBN\text{-}9\text{-}O)CdMe]_4$.[14] Several main group element boryloxides have also been structurally characterized including those containing $-OBAr_2$ (Li[9,12a] and Al[12b,13]), $-OB[CH(SiMe_3)_2]_2$ (Li),[31] and 9-BBN-9-O ligands (Al, In, Ga),[32] as well as $B(OEPh_3)_3$ (E = Sn,[17] Si[18]) and $PhB(OGePh_3)_2$.[18]

Reactions of Complex 4. Reaction of **3** with Cp_2ZrMe_2 in Et_2O gave a new product, $Cp_2Zr[OSi(O^tBu)_3]_2$ (**5**), that results (formally) from the elimination of "BMeO". Complex **5** was formed quantitatively as indicated by a ^1H NMR spectrum of the crude product mixture. Isolation of complex **5** was achieved by crystallization from the reaction mixture (Et_2O) at −78 °C in 84% yield. Addition of Et_2O to neat **4** at 25 °C also led to the quantitative formation of **5**, suggesting that **4** may be formed in the reaction of Cp_2ZrMe_2 with **3** in Et_2O but that it readily converts to **5** under these conditions (Scheme 1). The identity of complex **5** was confirmed by comparison of its ^1H NMR, ^{13}C NMR, and IR spectra to those of an authentic sample synthesized by the addition of 2 equiv of $HOSi(O^tBu)_3$ to a pentane solution of Cp_2ZrMe_2.[33] The thermolysis of **4** in benzene-d_6 at 80 °C (in a sealed J-Young NMR tube) also led to the formation of **5** (90% yield by ^1H NMR spectroscopy).

The solvent-induced conversion of **4** to **5** suggests the participation of a polar intermediate. This, coupled with the known ability of boryloxides to abstract alkyl groups from Lewis acidic centers,[32,34] leads us to propose an intramolecular methide transfer from Zr to B, with subsequent transfer of a tris(*tert*-butoxy)siloxide ligand from the resulting $\{OBMe[OSi(O^tBu)_3]_2\}^-$ group to the now cationlike Zr center. Elimination of "BMeO" from a $Zr-OB(Me)[OSi(O^tBu)_3]$ species would then form the observed product (**5**). Attempts to observe intermediates by performing thermolyses in the presence of a base (pyridine, MeCN) or upon dissolution of **4** in Et_2O/base mixtures led to the exclusive formation of **5**. Unfortunately, no intermediate species could be identified in the above reaction mixtures (by ^1H NMR spectroscopy) and no resonances were detected in their ^{11}B NMR spectra. On the basis of mass balance considerations, the boroxine $(MeBO)_3$ is a reasonable product that could account for the eliminated "BMeO" fragments from **4**. However, we were unable to detect this (or any other) boron-containing species by ^1H and ^{11}B NMR spectroscopy or by GC/MS analysis of reaction mixtures; hence, the fate of the boron upon conversion of **4** to **5** is unknown at this time. The formation of nonvolatile oligomeric or polymeric species is possible and would lead to severely broadened NMR resonances that could account for the difficulties encountered in locating the boron.

Conclusions

Syntheses of the new boron-based tris(*tert*-butoxy)siloxide species $^tBuOB[OSi(O^tBu)_3]_2$ (**1**), $B[OSi(O^tBu)_3]_3$ (**2**), and $HOB[OSi(O^tBu)_3]_2$ (**3**) have been achieved. Compounds **1** and **2** are efficient single-source molecular precursors that have been used to produce borosilicate xerogels (**BOSi2$_{xg}$** and **BOSi3$_{xg}$**, respectively) from nonpolar media utilizing the thermolytic molecular precursor method. **BOSi3$_{xg}$** is a high surface area borosilicate xerogel (590 $m^2\ g^{-1}$) with formula $BO_{1.5}{\cdot}3SiO_2$, while the xerogel **BOSi2$_{xg}$** ($BO_{1.5}{\cdot}2SiO_2$) has a smaller area (48 $m^2\ g^{-1}$). Use of $EO_{20}PO_{70}EO_{20}$ during the solution thermolyses of **1** and **2** resulted in formation of new xerogels (**BOSi2$_{epe}$** and **BOSi3$_{epe}$**, respectively) that did not have ordered mesostructures; however, these materials were mesoporous in nature and had moderately high surface areas (ca. 160 $m^2\ g^{-1}$).

(31) Beck, G.; Hitchcock, P. B.; Lappert, M. F.; MacKinnon, I. A. *Chem. Commun.* **1989**, 1312.

(32) Anulewicz-Ostrowska, R.; Lulinski, S.; Serwatowski, J. *Inorg. Chem.* **1999**, *38*, 3796.

(33) Original synthesis of **5**: reaction of 2 equiv of $HOSi(O^tBu)_3$ with Cp_2ZrMe_2 in pentane at 25 °C and subsequent crystallization from pentane at −78 °C (66%). Terry, K. W. Ph.D. Thesis, University of California at San Diego, 1993. Data for **5 are as follows**. Anal. Calcd for $C_{34}H_{64}O_8Si_2Zr$: C, 54.58; H, 8.62. Found: C 54.79; H, 8.33. IR (cm^{-1}): 3100 w br, 1386 m, 1362 s, 1240 m, 1215 m, 1192 s, 1050 vs br, 1022 s sh, 1000 s sh, 946 s, 910 w sh, 845 vw sh, 822 m sh, 802 s, 720 vw sh, 696 s, 645 w, 614 vw sh, 525 vw sh, 504 vw sh, 481 w sh, 454 w, 424 w sh, 386 w, 350 w, 326 w. ^1H NMR (benzene-d_6, 300 MHz): δ 1.46 (s, 54H, $Si(O^tBu)_3$), 6.43 (s, 10H, Cp_2Zr). $^{13}C\{^1H\}$ NMR (benzene-d_6, 75.5 MHz): δ 113.25 (s, Cp_2Zr), 72.08 (s, $SiOC(CH_3)_3$), 31.98 (s, $SiOC(CH_3)_3$).

(34) Synoradzki, L.; Boleslawski, M.; Lewinski, J. *J. Organomet. Chem.* **1986**, *284*, 1.

Compound **3** appears to be the first boronous acid to contain a siloxide group, and it is a rare example of an isolable boronous acid.[9,15] Apparently, the steric bulk of the tris(*tert*-butoxy)siloxide groups suppresses condensation reactions and permits the isolation of **3** in high yield. This species should prove to be a valuable ligand precursor for the synthesis of new (siloxy)boryloxide complexes. The use of such compounds as single-source molecular precursors to complex oxide materials, and as molecular models for oxide-supported metal species, will be reported soon. Initial reactivity studies of **3** with Cp_2ZrMe_2 demonstrate the clean formation of a (siloxy)boryloxide complex, $Cp_2Zr(Me)OB[OSi(O^tBu)_3]_2$ (**4**), with a unique crystal structure containing 18 independent molecules in its asymmetric unit.

The statistical analyses of the crystallographic data for **4** show a normal distribution for the metric parameters allowing a high degree of confidence, even from a not overly determined structure (i.e., low symmetry and low data redundancy). Often crystals are deemed to be of insufficient quality when large unit cells are found for low-symmetry space groups during crystallographic investigations. However, the structure of **4** clearly illustrates that such large unit cells can be real and provide accurate structures, although such cases are obviously rare. The extreme flexibility of B−O−X bond angles is illustrated here by the fact that, for the 18 unique molecules in the asymmetric unit of **4**, chemically identical B−O−Zr and B−O−Si angles each exhibit ranges covering more than 30°.

The chemistry of transition metal boryloxide species appears to be relatively unexplored and, given the recently reported interesting catalytic activity of aluminum boryloxides,[12b,13] may provide access to new reactive and potentially catalytic species. Initial reactivity studies of **4** suggest that the Zr−CH_3 and Zr−O−B linkages are highly reactive and easily cleaved, even upon simple dissolution in Et_2O. Further investigations of the reactivity of $HOB[OSi(O^tBu)_3]_2$ with various transition and main group metal species are currently underway.

Experimental Section

General Methods. All synthetic manipulations were performed under an atmosphere of nitrogen using standard Schlenk techniques and/or a Vacuum Atmospheres drybox, unless noted otherwise. All solvents used were distilled from sodium/ benzophenone, potassium/ benzophenone, sodium, or calcium hydride as appropriate. The solution NMR spectra were recorded at ambient temperature using a Bruker AMX300 spectrometer at 300 (^{1}H) MHz, a Bruker AM400 spectrometer at 400 (^{1}H) or 100.6 (^{13}C) MHz, or a Bruker DRX500 spectrometer at 160.4 (^{11}B) MHz. Chemical shifts are reported in ppm relative to tetramethylsilane (^{1}H and ^{13}C) and BF_3·Et_2O (^{11}B). Benzene-d_6, vacuum transferred from a Na/K alloy, was used as the solvent for all NMR studies. Infrared spectra were recorded using a Mattson Infinity Series FTIR spectrometer with all samples being pressed into KBr disks. Thermal analyses were performed using a TA Instruments SDT 2960 integrated thermogravimetric/ differential scanning calorimetric analyzer (TGA/DSC). N_2 porosimetry was performed using a Quantochrome Autosorb 1 surface area analyzer with all samples heated at 120 °C for a minimum of 12 h prior to measurement. TEM images were acquired using a JEOL 200cx electron microscope operating at an accelerating voltage of 200 kV. Samples for TEM analyses were prepared via deposition using a pentane suspension of finely ground material on a "lacey carbon" copper grid obtained from Ted Pella Inc. X-ray powder diffraction data were obtained using a Siemens D5000 diffractometer operating with $\theta-2\theta$ geometry at room temperature. The PXRD data were collected using Cu Kα radiation ($\lambda = 1.5406$ Å). Collection times of 1.5 or 5.0 s and step sizes of 0.02 or 0.01° were used for high- or low-angle measurements, respectively. Elemental analyses were performed by the College of Chemistry Micro-Mass Facility at the University of California, Berkeley, CA. $B(O^tBu)_3$ was purchased from Gelest and used as received, the block copolymer $EO_{20}PO_{70}EO_{20}$ (Pluronic 123, $M_{av} = 5800$) was a generous gift from BASF (Mt. Olive, NJ), and $HOSi(O^tBu)_3$[35] and Cp_2ZrMe_2[36] were prepared by literature procedures.

^{t}BuOB[OSi(O^{t}Bu)$_3$]$_2$ (1). A neat mixture of $B(O^tBu)_3$ (2.436 g, 10.58 mmol) and $HOSi(O^tBu)_3$ (5.598 g, 21.17 mmol) was heated at 80 °C for 18 h in a Schlenk tube. The Schlenk tube was cooled to room temperature, and the volatile materials were removed in vacuo leaving a colorless solid. The solid was dissolved in toluene (20 mL), and acetonitrile (5 mL) was subsequently added. The resulting solution was stored at −30 °C for 24 h, yielding colorless platelike crystals. The crystals were washed with acetonitrile to yield 5.074 g (8.31 mmol) of analytically pure **1** (79%). Anal. Calcd for $C_{28}H_{63}BO_9Si_2$: C, 55.06; H, 10.40. Found: C, 55.10; H, 10.42. IR (cm^{-1}): 2977 vs, 2933 m, 2902 w, 2876 w, 1474 m, 1414 m, 1389 s, 1366 s, 1341 s, 1244 m, 1194 s, 1069 vs, 1027 m, 879 m, 832 m, 704 m, 675 w, 622 w, 514 m, 483 m, 425 w. ^{1}H NMR (300 MHz): δ 1.48 (s, 9 H, BO^t*Bu*), 1.47 (s, 54 H, Si(O^t*Bu*)$_3$). ^{13}C{^{1}H} NMR (100.6 MHz): δ 72.92 (s, Si(O*C*(CH$_3$)$_3$), 72.62 (s, BO*C*(CH$_3$)$_3$), 31.75 (s, Si(OC(*C*H$_3$)$_3$), 30.39 (s, BOC(*C*H$_3$)$_3$). ^{11}B{^{1}H} NMR (160.4 MHz): δ 12.9 (s, br). Mp: ∼72 °C. Bp: ∼170 °C.

B[OSi(O^{t}Bu)$_3$]$_3$ (2). To a mixture of $HOSi(O^tBu)_3$ (4.197 g, 15.9 mmol) and $B(O^tBu)_3$ (1.218 g, 5.29 mmol) in a Schlenk tube was added toluene (5 mL). The tube was heated at 80 °C, and the reaction mixture was magnetically stirred for 24 h. Subsequent cooling to room temperature and removal of the volatile materials in vacuo left a colorless solid. The resulting solid was then dissolved in toluene (10 mL), and acetonitrile (2.5 mL) was added. Analytically pure colorless needlelike crystals were obtained after storage at −30 °C for 24 h and subsequent washing of the isolated crystals with acetonitrile (61% yield; 2.582 g, 3.22 mmol). Anal. Calcd for $C_{36}H_{81}BO_{12}Si_3$: C, 53.98; H, 10.19. Found: C, 53.79; H, 10.15. IR (cm^{-1}): 2976 vs, 2932 m, 2907 w, 2875 vw, 1474 vw, 1388 m, 1366 s, 1244 m, 1194 s, 1075 vs, 1028 m, 881 m, 832 m, 704 m, 616 w, 518 m, 493 w. ^{1}H NMR (300 MHz): δ 1.50 (s, 81 H, Si(O^t*Bu*)$_3$). ^{13}C{^{1}H} NMR (100.6 MHz): δ 73.06 (s, Si(O*C*(CH$_3$)$_3$), 31.96 (s, Si(OC(*C*H$_3$)$_3$). ^{11}B{^{1}H} NMR (160.4 MHz): δ 12.9 (s, br). Mp: ∼162 °C. Bp: ∼257 °C.

BOSi2$_{xg}$ and BOSi3$_{xg}$. Representative solution thermolyses to form **BOSi2$_{xg}$** and **BOSi3$_{xg}$** were carried out as follows: A thick-walled pyrolysis tube was charged with a toluene (8.0 mL) solution of **1** (1.000 g, 1.637 mmol) or **2** (1.311 g, 1.637 mmol) in a drybox. To this solution was added $AlCl_3$ (0.002 g, 0.016 mmol, 1 mol %) in solid form. The tube was flame-sealed after three freeze−pump−thaw cycles and placed in a preheated oven at 180 °C. A clear monolithic gel was evident after ∼45 min. The tube was heated for an additional 36 h to ensure complete conversion. After this heating period the tube containing the gel was cooled to room

(35) Abe, Y.; Kijima, I. *Bull. Chem. Soc. Jpn.* **1969**, *42*, 1118.
(36) Hunter, W. E.; Hrincr, D. C.; Bynum, R. V.; Pentilla, R. A.; Atwood, J. L. *Organometallics* **1983**, *2*, 750.

temperature and opened. The gel was transferred to a Schlenk tube under N_2 and dried under flowing N_2 for 5 days at 25 °C giving the xerogel **BOSi2$_{xg}$** or **BOSi3$_{xg}$**. The xerogels were further dried in vacuo at 25 °C for 24 h and finally at 120 °C in vacuo for an additional 24 h. The mass of **BOSi2$_{xg}$** obtained was 0.234 g (23.4% ceramic yield), and that of **BOSi3$_{xg}$** was 0.339 g (25.8%). The xerogel pieces were then ground to a fine powder and calcined at 500 °C under O_2.

BOSi2$_{epe}$ and BOSi3$_{epe}$. Representative solution thermolyses in the presence of $EO_{20}PO_{70}EO_{20}$ were carried out as follows: A thick-walled pyrolysis tube was charged with a toluene solution (6.0 mL) of **1** (0.400 g, 0.655 mmol) or **2** (0.500 g, 0.624 mmol) and $EO_{20}PO_{70}EO_{20}$ (0.300 g) in a drybox. To this solution was added $AlCl_3$ (1 mg, 1 mol %) in solid form. The tube was flame-sealed after three freeze−pump−thaw cycles and treated as described previously except that the as-synthesized gel was washed several times with hexanes (to extract any free polymer) prior to the drying process. After calcination at 550 °C for 8 h (to remove any remaining block copolymer) the xerogels **BOSi2$_{epe}$** (0.083 g, 21%) or **BOSi3$_{epe}$** (0.109 g, 22%) were obtained.

HOB[OSi(O^{t}Bu)$_3$]$_2$ (3). To a magnetically stirring solution of **1** (0.679 g, 1.112 mmol) in benzene (10 mL) was added dropwise via syringe H_2O (20 μL, 1.112 mmol) in a Schlenk tube. The reaction mixture was stirred at 25 °C for 1 h and was subsequently cooled to 0 °C using an ice bath. The reaction mixture solidified due to freezing of the benzene. The tube was evacuated while cold resulting in the removal of the benzene (via lyophilization) leaving an opaque powder consisting of **3** and a small amount of **2** as an impurity (ca. 5%). Subsequent sublimation of this powder at 50 °C in vacuo (ca. 0.01 mmHg) resulted in isolation of analytically pure **3** in 86% yield (0.528 g, 0.952 mmol). Anal. Calcd for $C_{24}H_{55}BO_9Si_2$: C, 51.97; H, 9.99. Found: C, 51.93; H, 9.96. IR (cm^{-1}): 3223 br, 2977 vs, 2934 m, 2910 w, 2876 w, 1474 m, 1423 m, 1390 m, 1367 s, 1339 m, 1245 m, 1194 s, 1068 vs, 1025 m, 877 m, 832 m, 705 s, 618 w, 516 m, 489 m. 423 w. ^{1}H NMR (300 MHz): δ 5.71 (s, 1 H, BO*H*), 1.41 (s, 54 H, Si(O^t*Bu*)$_3$). ^{13}C{^{1}H} NMR (100.6 MHz): δ 73.39 (s, Si(O*C*(CH$_3$)$_3$), 31.48 (s, Si(OC(*C*H$_3$)$_3$). ^{11}B{^{1}H} NMR (160.4 MHz): δ 15.4 (s, br). Mp: 57 °C. Bp: ∼240 °C.

Cp$_2$Zr(Me)OB[OSi(O^{t}Bu)$_3$]$_2$ (4). To a solid mixture of Cp_2ZrMe_2 (0.046 g, 0.184 mmol) and HOB[OSi(O^{t}Bu)$_3$]$_2$ (0.102 g, 0.184 mmol) in a Schlenk tube was added pentane (2 mL) with magnetic stirring at 25 °C. The evolution of a gas was observed. After 30 min, the reaction mixture was concentrated in vacuo to 1 mL and stored at −78 °C for 24 h. Analytically pure colorless crystals of **4** were isolated in 90% yield (0.127 g, 0.166 mmol). Anal. Calcd for $C_{35}H_{67}BO_9Si_2Zr$: C, 53.21; H, 8.55. Found: C, 53.29; H, 8.67. IR (cm^{-1}): 2975 vs, 2931 m, 2900 w sh, 2874 w, 1474 w, 1458 w, 1419 w, 1389 m, 1366 s, 1339 m, 1243 m, 1193 s, 1066 vs, 1025 s, 976 w, 861 vw, 831 w, 801 m, 748 w, 704 m, 675 w, 616 w, 517 vw, 491 w, 459 w, 428 w. ^{1}H NMR (400 MHz): δ 6.07 (s, 10 H, *Cp*$_2$Zr), 1.48 (s, 54 H, Si(O^t*Bu*)$_3$), 0.49 (s, 3 H, ZrC*H*$_3$). ^{13}C{^{1}H} NMR (100.6 MHz): δ 111.63 (s, *Cp*$_2$Zr), 72.80 (s, SiO*C*(CH$_3$)$_3$), 31.86 (s, Si(OC(*C*H$_3$)$_3$), 24.18 (s, ZrCH$_3$). ^{11}B{^{1}H} NMR (160.4 MHz): δ 13.0 (s, br). Mp: ∼30 °C (d).

X-ray Structure Determinations. Each crystal was mounted on a quartz fiber using Paratone N hydrocarbon oil. In the case of **4**, the crystals were kept cold at all times (−30 °C) to minimize reaction with/dissolution in the Paratone oil. All measurements were made on a SMART CCD area detector with graphite-monochromated Mo Kα radiation and a crystal to detector distance of 60.0 cm. Data for **1** and **4** were integrated using the program SAINT (SAX Area-Detector Integration Program, V5.04; Bruker, 1995) and were corrected for Lorentz and polarization effects. The data were analyzed for agreement and possible absorption using XPREP (part of the SHELXTL Crystal Structure Determination suite of programs; Bruker, 1995). An empirical absorption correction based upon comparison of redundant and equivalent reflections was applied using SADABS (Siemens Area Detector Absorption Corrections; Sheldrick, G. M., 1996). The structure of **1** was solved by direct methods and refined using Fourier techniques (based upon F^2) with all calculations performed using the SHELXTL crystallographic software package (Sheldrick, G. M. SHELXTL, V5.03; Bruker, 1994). The structure of **4** was also solved by direct methods and refined routinely (F^2); however, a blocking strategy was applied due to the large number of refined parameters (7648). The first block involved refinement of all 18 Zr atoms, and each subsequent block consisted of one of the independent molecules (including their respective Zr atoms). During the solution process, three potential pseudo-inversion centers were located. The true center was selected by inspection of the Zr and Si positions and confirmed by refinement statistics and the complete solution and refinement of the structure. The molecules in the asymmetric unit of **4** lie in three chains of six molecules that run parallel to the [20$\bar{1}$] plane within the lattice. All non-hydrogen and non-boron atoms that did not exhibit disorder were refined with anisotropic thermal parameters for both **1** and **4**, and the hydrogen atoms were included in calculated idealized positions but not refined.

Acknowledgment. This work was supported by the Director, Office of Energy Research, Office of Basic Energy Sciences, Chemical Sciences Division, of the U.S. Department of Energy under Contract No. DE-AC03-76SF00098. We thank A. Stacy for the use of instrumentation (PXRD).

Supporting Information Available: Crystallographic information files (CIF) for **1** and **4**. This material is available free of charge via the Internet at http://pubs.acs.org.

IC0205482